This article has been accepted for publication in a future issue of this journal, but has not been fully edited. Content may change prior to final publication. Citation information: DOI 10.1109/TSP.2015.2460221, IEEE Transactions on Signal Processing

Response Vector Constrained Robust LCMV Beamforming Based on Semidefinite Programming

Jingwei Xu, Guisheng Liao, *Member, IEEE*, Shengqi Zhu, *Member, IEEE*, and Lei Huang, *Senior Member, IEEE*

Abstract

Although linearly constrained minimum variance (LCMV) beamforming is robust against imprecise target information, it usually leads to relatively high sidelobe and distorted mainlobe which would induce a high false alarm probability. To circumvent this problem, this work devises a novel robust LCMV beamforming approach by utilizing response vector optimization. It intends to find the optimal response vector in lieu of the all-one response vector in traditional LCMV beamformer. The proposed robust beamformer is first formulated as a non-convex quadratically constrained quadratic programming problem, and then transformed into a semidefinite programming problem which can be efficiently and exactly solved. The proposed beamformer not only improves the performance in terms of signal-to-interference-plus-noise ratio substantially, but also possesses low sidelobe and well-maintained mainlobe. Moreover, since the response vector is quite small in size, the complexity of calculating the optimal response vector is negligible. Additionally, the proposed beamformer is also extended to two-dimensional space-time adaptive processing. Simulation results are presented to demonstrate the superiority of the proposed approach.

Index Terms

Robust adaptive beamforming, linearly constrained minimum variance beamformer, response vector optimization, quadratically constrained quadratic programming, semidefinite programming.

I. Introduction

Adaptive digital beamforming (DBF) is a classical approach for target detection, interference cancellation and direction-of-arrival (DOA) estimation. The adaptive beamformer in spatial-temporal domains, namely, the space-time

This work was supported by the National Nature Science Foundation of China (NSFC) (Grants 61231017 and 91438106).

J. Xu, G. Liao, and S. Zhu are with the National Laboratory of Radar Signal Processing, Xidian University, Xi'an, Shaanxi, 710071, China. (e-mail: xujingwei1987@163.com; gsliao@xidian.edu.cn; zhushengqi8@163.com).

L. Huang is with the College of Information Engineering, Shenzhen University, Shenzhen, China. (e-mail: dr.lei.huang@ieee.org).

adaptive processing (STAP), is capable of jointly exploiting multiple receive elements and multiple transmitted pulses in spatial-temporal domains to suppress deleteriously correlated clutter and interference [1]. Therefore, the adaptive beamforming has been used in many areas, such as radar, sonar, wireless communication, medical imaging and so on. Note that DBF is applied only in spatial domain while STAP is performed in joint spatial and temporal domains. The STAP includes the DBF as a special case when the pulse number is equal to one. Therefore, the structures of the steering vectors of DBF and STAP are different, which induces distinguishable approaches in practical applications. Usually, the adaptive beamformer is designed according to some criteria, such as the minimum variance distortionless response (MVDR), minimum mean-squared error (MMSE) and maximum signal-to-noise ratio (SNR). As a popular beamformer, Capon approach is developed upon the assumption that the desired target signal is absent from the training data and the knowledge of the target direction is known accurately [2]. Under this condition, it enjoys both high resolution and good interference suppression.

It is well known that the traditional Capon method is quite sensitive to errors, thereby calling for robust adaptive beamforming approach in practical applications. Usually, the small sample support, imprecise knowledge of the signal steering vector and training data corrupted by the target signal are the main causes of performance degradation in adaptive beamforming. The performance degradation also results from the mismatch between the assumed and actual steering vectors, source spreading, imperfect array calibration, distorted antenna shape and extended target in high resolution radars. The performance degradation becomes more severe in STAP due to the fact that the spatial and temporal frequencies of clutter are coupled in spatial-temporal domains and the characteristic of clutter is typical non-homogeneity in phased-array radar [3]. That is to say, the training data does not satisfy the independent and identically distributed (IID) condition. Besides, the training data may also be corrupted by other moving targets, especially in heavy traffic or group target circumstance [4], i.e., a number of closely spaced targets moving in a coordinated fashion. This eventually results in inter-target nulling phenomenon.

Various approaches have been developed to address the robust beamforming. Diagonal loading technique and its variants are quite efficient in enhancing the robustness of the Capon beamformer [5]–[7]. However, the limitation of diagonal loading method is that it cannot provide any guidance to accurately determine the diagonal loading factor. Several worst-case optimization beamformers were proposed in [8]–[10], which have been proved to be equivalent to each other and belong to the class of diagonal loading approach with accurate relationship between the diagonal loading factor and uncertainty-set. The doubly constrained robust Capon beamforming method [11], [12] and the probabilistically constrained robust adaptive beamforming technique [13] are the variants of the worst-case-based approach in solving practical problems. In [14], a steering vector estimation based robust adaptive beamforming technique is presented, which does not require any assumptions on the norm of steering vector error or its probability distribution. In order to find the actual steering vector of the MVDR beamformer, the output power is maximized under some constraint in [14], which is based on the observation that interference can be effectively suppressed by the optimal adaptive weight of MVDR beamformer and thus the output power mainly consists of the target signal. It is revealed in [15], [16] that the eigenspace-based beamformers are of robustness against target steering vector errors. However, they rely on the knowledge of source number which turns out to be

This article has been accepted for publication in a future issue of this journal, but has not been fully edited. Content may change prior to final publication. Citation information: DOI 10.1109/TSP.2015.2460221, IEEE Transactions on Signal Processing

unknown and needs to be estimated [17]–[19]. Moreover, they become rather ineffective when the dimension of the signal-plus-interference subspace is high or the SNR is low because the signal and noise subspaces swap with high probability in these cases. Another popular approach is the so-called linearly constrained minimum variance (LCMV) beamformer [20]–[24], which imposes several linear constraints when minimizing the output variance, thus offering robustness against signal steering vector mismatch. The LCMV method can broaden the mainlobe or notch of the beampattern while maintaining the output of the target at the expense of degree-of-freedom (DOF) consumption. Indeed, it is inefficient in terms of sidelobe suppression, thus leading to poor performance, especially in extended clutter environment. A phase response constrained LCMV beamformer has been proposed in [25], which yields a lower sidelobe of the beampattern than the traditional LCMV beamformer. In [26], linear constraints are used in robust Capon beamforming to handle arbitrary array steering vector errors, which coincides with the LCMV beamformer. In [27], a robust adaptive beamformer was proposed using two quadratic constraints to force the magnitude response of two constrained points to exceed unity. This method can be taken as an LCMV beamformer with its response vector further optimized. Constraints on array magnitude response are also considered in [28]–[30], yielding robust adaptive beamformers which are able to flexibly control the robust response region with specified beamwidth and response ripple. In [28], the optimization of an adaptive beamformer is reformulated as a linear programming problem by transforming the array output covariance and magnitude response into linear functions of the autocorrelation sequence of the array weight. In [29], a robust adaptive beamformer is established by exploiting the semidefinite programming (SDP), whereby the beamformer is also cast as a linear programming problem. The magnitude response constraints and conjugate symmetric structure of the array weight are utilized to derive a robust beamformer without any relaxation or approximation [31], which substantially improves the performance. In [32], a covariance matrix tapering method has been proposed to overcome the pattern distortion resulting from insufficient sample support or nonstationary interference. The covariance matrix tapering for STAP radar can provide robust clutter cancellation. To alleviate the performance degradation when uncertainty appears in the DOA and Doppler frequency, a robust direct data domain STAP method has been proposed in [33], which considers a mismatch between the assumed and actual steering vectors and improves the performance of STAP radar.

Although the traditional LCMV beamformer is robust against imprecise target DOA estimations, its performance degradation is evident due to the relatively high sidelobe and distorted mainlobe of the beampattern, especially in nonstationary environment. In this paper, we devise a robust LCMV beamformer based on response vector optimization (RVO), called RVO-LCMV beamformer, which provides superiority in robustness as well as output signal-to-interference-plus-noise ratio (SINR). To this end, we first establish the objective function with respect to the response vector and then minimize the output power of the LCMV beamformer under the constraint that the mainlobe response exceeds unity to maintain the mainlobe of the beampattern. In the sequel, the constraints are imposed on the response vector, yielding a non-convex quadratically constrained quadratic programming (QCQP) problem. To solve this problem, we transform the QCQP problem into a relaxed SDP problem. Note that the exact equivalence between the relaxed SDP based beamformer and original QCQP based beamformer relies on the existence of a rank-one constraint on the optimal semidefinite matrix. As a result, an approximate solution is

This article has been accepted for publication in a future issue of this journal, but has not been fully edited. Content may change prior to final publication. Citation information: DOI 10.1109/TSP.2015.2460221, IEEE Transactions on Signal Processing

provided, which approaches the optimal solution in probability one. Compared with the state-of-the-art techniques, the proposed method can suppress the sidelobe efficiently and maintain the mainlobe properly. Besides, the proposed method significantly reduces the computational complexity as the response vector is usually small in size.

The paper is organized as follows. In Section II, the signal models are introduced accommodating the DBF and STAP radars. In Section III, the RVO-LCMV beamformer is devised, and the non-convex original QCQP problem is transformed into a relaxed SDP problem. The performance analysis of the proposed method is conducted in Section IV. Numerical results are presented in Section V. Finally, conclusions are presented in Section VI.

II. Problem Formulation

We consider a monostatic linear array radar with N omni-directional antenna elements. The narrowband signal received by the array can be expressed as

$$\mathbf{x}(t) = \mathbf{s}(t) + \mathbf{i}(t) + \mathbf{n}(t) \tag{1}$$

where $\mathbf{s}(t)$, $\mathbf{i}(t)$ and $\mathbf{n}(t)$ denote the target signal, jamming interference and/or ground clutter, and white Gaussian noise, respectively. For DBF, the desired signal can be written as $\mathbf{s}(t) = s(t)\mathbf{a}_s$, where $s(t)$ is the signal waveform and $\mathbf{a}_s$ is the spatial steering vector. For STAP, K coherent pulses are collected and stacked into NK-dimensional space-time snapshots, i.e., $\mathbf{s}(t) = s(t)\mathbf{a}_{s-t} = s(t)\mathbf{a}_t \otimes \mathbf{a}_s$, where $\otimes$ denotes the Kronecker product and $\mathbf{a}_t$ is the temporal steering vector.

The output of the beamformer is the weighted summation of the received data, i.e.,

$$y(t) = \mathbf{w}^{\mathrm{H}}\mathbf{x}(t) \tag{2}$$

where the superscript $^{\mathrm{H}}$ denotes Hermitian transpose operator and $\mathbf{w}$ is the complex-valued weight. The weight can be determined by the MVDR criterion, that is,

$$\min_{\mathbf{w}} \mathbf{w}^{\mathrm{H}}\mathbf{R}\mathbf{w} \quad \text{s.t.} \quad \mathbf{w}^{\mathrm{H}}\mathbf{a} = 1 \tag{3}$$

where $\mathbf{R}$ is the interference/clutter-plus-noise covariance matrix, $\mathbf{a} = \mathbf{a}_s$ for DBF and $\mathbf{a} = \mathbf{a}_{s-t}$ for STAP. In practical implementations, the covariance matrix is usually obtained by averaging the outer-product of the snapshot in range:

$$\hat{\mathbf{R}} = \frac{1}{L}\sum_{l=1}^{L} \mathbf{x}_l\mathbf{x}_l^{\mathrm{H}} \tag{4}$$

where L is the number of snapshots. According to the well-known RMB rule [34], the required amount of the snapshots to well estimate the covariance matrix is more than twice the number of antennas for DBF when the observations are IID. For STAP, on the other hand, this amount is more than twice NK provided that the observed data are IID. However, the nonstationary and non-homogeneity of the clutter will seriously deviate from the underlying IID assumption. Besides, the information of the target under test is usually not accurate. These errors considerably degrade the performance of the sample matrix inverse (SMI) based MVDR (SMI-MVDR) beamformer.

This article has been accepted for publication in a future issue of this journal, but has not been fully edited. Content may change prior to final publication. Citation information: DOI 10.1109/TSP.2015.2460221, IEEE Transactions on Signal Processing

To overcome this problem, an LCMV beamformer was proposed in [20] by imposing multiple unity-gain constraints for a small spread of angles and/or Doppler frequencies around the assumed angle and/or Doppler frequencies.

$$\min_{\mathbf{w}} \mathbf{w}^{\mathrm{H}}\hat{\mathbf{R}}\mathbf{w} \quad \text{s.t.} \quad \mathbf{w}^{\mathrm{H}}\mathbf{C} = \mathbf{f}^{\mathrm{T}} \tag{5}$$

where $\mathbf{C}$ is the constraint matrix consisting of M spatial steering vectors corresponding to the constrained directions (or M space-time steering vectors corresponding to the constrained DOAs and Doppler frequencies), and $\mathbf{f}$ is the all-one response vector with each element specifying the desired unity-gain response. The solution to (5) is

$$\mathbf{w} = \hat{\mathbf{R}}^{-1}\mathbf{C}\left(\mathbf{C}^{\mathrm{H}}\hat{\mathbf{R}}^{-1}\mathbf{C}\right)^{-1}\mathbf{f}. \tag{6}$$

As pointed out above, nevertheless, the traditional LCMV beamformer yields relatively high sidelobe of the beampattern, thereby being more sensitive to the unknown interference. Another disadvantage of the traditional LCMV beamformer is that its mainlobe is not well maintained [26]. In STAP applications, for example, the high sidelobe and distorted mainlobe induce severe performance degradation [3]. In order to improve the performance of LCMV beamformer in practical situations, we will devise an optimal response vector in lieu of the all-one response vector in the following section.

III. Robust RVO-LCMV Beamforming Method

As aforementioned, the response vector in the traditional LCMV beamformer is usually set as an all-one vector to guarantee unity gains. Actually, this kind of response vector is mismatched with the constraint matrix $\mathbf{C}$. Consequently, the traditional LCMV beamformer suffers from dramatical performance degradation due to high sidelobe and distorted mainlobe. To circumvent this problem, the response vector in (5) is further refined in this section. The motivation comes from the observation that the sidelobe of the beampattern is lowered when the phase of the response vector is considered [25], [31]. Therefore, we are able to achieve performance improvement by replacing the response vector with an optimal one.

Recalling that each element of the response vector is complex-valued, the LCMV beamformer in (5) can be rewritten as

$$\min_{\mathbf{w}} \mathbf{w}^{\mathrm{H}}\hat{\mathbf{R}}\mathbf{w} \quad \text{s.t.} \quad \mathbf{w}^{\mathrm{H}}\mathbf{C} = \mathbf{u}^{\mathrm{T}} \tag{7}$$

where $\mathbf{u} = (u_1, u_2, \cdots, u_M)^{\mathrm{T}}$ is the $M \times 1$ complex-valued response vector. The adaptive weight takes the similar form as (6), that is,

$$\mathbf{w} = \hat{\mathbf{R}}^{-1}\mathbf{C}\left(\mathbf{C}^{\mathrm{H}}\hat{\mathbf{R}}^{-1}\mathbf{C}\right)^{-1}\mathbf{u}^{*} \tag{8}$$

where the superscript * is the conjugate operator. Substituting (8) into the objective function of (7) yields

$$f(\mathbf{u}) = \mathbf{u}^{\mathrm{T}}\left(\mathbf{C}^{\mathrm{H}}\hat{\mathbf{R}}^{-1}\mathbf{C}\right)^{-1}\mathbf{u}^{*}. \tag{9}$$

Note that $\mathbf{P} = \left(\mathbf{C}^{\mathrm{H}}\hat{\mathbf{R}}^{-1}\mathbf{C}\right)^{-1}$ is a Hermitian matrix, i.e., $\mathbf{P} = \mathbf{P}^{\mathrm{H}}$. Moreover, because $\hat{\mathbf{R}}$ is a positive semidefinite matrix and $\mathbf{C}$ is full column rank, $\mathbf{P}$ is a positive semidefinite matrix, i.e., $\mathbf{P} \succeq 0$. In order to maintain the mainlobe

This article has been accepted for publication in a future issue of this journal, but has not been fully edited. Content may change prior to final publication. Citation information: DOI 10.1109/TSP.2015.2460221, IEEE Transactions on Signal Processing

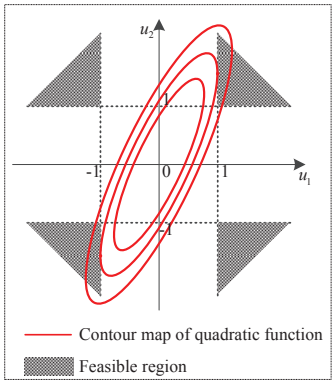

Fig. 1: Illustration of the solution to Problem (12)

of the beampattern, we assume that the absolute value of each element of the response vector exceeds unity. Thus, we obtain

$$\min_{\mathbf{u}} \mathbf{u}^{\mathrm{T}}\mathbf{P}\mathbf{u}^{*} \quad \text{s.t.} \quad |u_m| \geq 1, \quad m = 1, 2, \cdots, M. \tag{10}$$

We define a matrix $\mathbf{B}_m = \{b_{p,q}\}$, where $b_{p,q}$ is 1 if and only if $p = m$ and $q = m$, otherwise, $b_{p,q}$ is 0, that is,

$$\mathbf{B}_m = \left\{ b_{p,q} \left| \begin{array}{l} b_{p,q} = 1, \ p = m \text{ and } q = m \\ b_{p,q} = 0, \ p \neq m \text{ or } q \neq m \end{array} \right. \right\}. \tag{11}$$

Therefore, (10) can be further rewritten as

$$\min_{\mathbf{u}} \mathbf{u}^{\mathrm{T}}\mathbf{P}\mathbf{u}^{*} \quad \text{s.t.} \quad \mathbf{u}^{\mathrm{H}}\mathbf{B}_m\mathbf{u} \geq 1, \ m = 1, 2, \cdots, M. \tag{12}$$

This is a non-convex QCQP problem because the feasible set is outside of the constrained ellipsoid. The problem (12) is different from those in [28]–[31]. The variable of the proposed approach is the response vector which is very small in size. To illustrate the solution to (12), a response vector consisting of two components is depicted in Fig. 1. It is seen that the feasible set of (12) is the quadrants in the four corners, which is non-convex.

The problem in (12) can be expressed in higher dimension subspace as a SDP problem [35]. In particular, the objective function can be written as

$$\mathbf{u}^{\mathrm{H}}\mathbf{P}\mathbf{u} = \mathrm{tr}\left\{\mathbf{u}^{\mathrm{H}}\mathbf{P}\mathbf{u}\right\} = \mathrm{tr}\left\{\mathbf{P}\mathbf{U}\right\} \tag{13}$$

where $\mathrm{tr}(\cdot)$ denotes the trace operator and the property $\mathrm{tr}\{\mathbf{AB}\} = \mathrm{tr}\{\mathbf{BA}\}$ has been used. The matrix $\mathbf{U}$ is defined as $\mathbf{U} = \mathbf{u}\mathbf{u}^{\mathrm{H}}$ which is Hermitian positive semidefinite, i.e., $\mathbf{U} \succeq 0$. It is clear that the rank of $\mathbf{U}$ is one, i.e., $\mathrm{rank}\{\mathbf{U}\} = 1$. Similarly, the constraint in (12) can also be transformed as

$$\mathrm{tr}\left\{\mathbf{B}_m\mathbf{U}\right\} \geq 1, \quad m = 1, 2, \cdots, M. \tag{14}$$

Thus, Problem (12) amounts to the following problem

$$\min_{\mathbf{U}} \mathrm{tr}\left\{\mathbf{P}\mathbf{U}\right\} \ \text{s.t.} \left\{ \begin{array}{l} \mathrm{tr}\left\{\mathbf{B}_m\mathbf{U}\right\} \geq 1, m = 1, 2, \cdots, M \\ \mathbf{U} \succeq 0, \quad \mathrm{rank}(\mathbf{U}) = 1 \end{array} \right. \tag{15}$$

This article has been accepted for publication in a future issue of this journal, but has not been fully edited. Content may change prior to final publication. Citation information: DOI 10.1109/TSP.2015.2460221, IEEE Transactions on Signal Processing

From (15), we can see that this problem is linear with respect to the matrix variable $\mathbf{U}$. However, the rank-one constraint is non-convex. This is because the introduction of two rank-one matrix will yield a rank-two matrix if these two matrices do not share the same range. Generally, it is difficult to solve a non-convex problem. However, this problem can be solved by using semidefinite relaxation, i.e., dropping the rank-one constraint. Thus, a relaxed SDP problem is obtained as [35], [39]

$$\min_{\mathbf{U}} \operatorname{tr}\{\mathbf{P}\mathbf{U}\} \ \text{ s.t.} \begin{cases} \operatorname{tr}\{\mathbf{B}_m\mathbf{U}\} \geq 1, m = 1, 2, \cdots, M \\ \mathbf{U} \succeq 0 \end{cases} \tag{16}$$

In summary, the robust LCMV beamforming is expressed as a problem aiming at finding the optimal response vector. Moreover, we have converted the original QCQP problem in (12) into a relaxed SDP problem in (16) which can be easily and exactly solved using the standard and highly efficient interior point method software tools [36]. In general, the semidefinite relaxation can only be used to obtain a lower bound for the optimal objective function and provide an approximate solution to the original problem. If the rank of $\mathbf{U}$ equals to one, then the optimal solution can be determined exactly. However, the rank of $\mathbf{U}$ can be larger than one. Thus, we should find the proper approach to generate the rank-one $\mathbf{U}$. Further discussions on the rank-one approximation will be provided in section IV.A.

Indeed, Problem (16) can also be implemented by utilizing the corresponding real and imaginary components of the complex-valued response vector. Defining

$$\hat{\mathbf{u}} = \begin{bmatrix} \operatorname{Re}\{\mathbf{u}\} \\ \operatorname{Im}\{\mathbf{u}\} \end{bmatrix} \tag{17a}$$

$$\hat{\mathbf{P}} = \begin{bmatrix} \operatorname{Re}\{\mathbf{P}\} & \operatorname{Im}\{\mathbf{P}\} \\ -\operatorname{Im}\{\mathbf{P}\} & \operatorname{Re}\{\mathbf{P}\} \end{bmatrix} \tag{17b}$$

$$\hat{\mathbf{B}}_m = \begin{bmatrix} \mathbf{B}_m & 0 \\ 0 & \mathbf{B}_m \end{bmatrix} \tag{17c}$$

we can obtain

$$\min_{\hat{\mathbf{u}}} \hat{\mathbf{u}}^{\mathrm{T}}\hat{\mathbf{P}}\hat{\mathbf{u}} \ \text{ s.t. } \ \hat{\mathbf{u}}^{\mathrm{T}}\hat{\mathbf{B}}_m\hat{\mathbf{u}} \geq 1, \quad m = 1, 2, \cdots, M. \tag{18}$$

By using the similar procedure aforementioned, the QCQP problem in (18) can be reformulated as a relaxed SDP problem, that is,

$$\min_{\hat{\mathbf{U}}} \operatorname{tr}\left\{\hat{\mathbf{P}}\hat{\mathbf{U}}\right\} \ \text{ s.t.} \begin{cases} \operatorname{tr}\left\{\hat{\mathbf{B}}_m\hat{\mathbf{U}}\right\} \geq 1, m = 1, 2, \cdots, M \\ \hat{\mathbf{U}} \succeq 0 \end{cases} \tag{19}$$

where $\hat{\mathbf{U}} = \hat{\mathbf{u}}\hat{\mathbf{u}}^{\mathrm{H}}$. Since $\hat{\mathbf{u}}$ is a real-valued vector, $\hat{\mathbf{U}}$ is symmetric positive semidefinite. Note that after solving the optimization problem (19), a suboptimal solution $\hat{\mathbf{u}}$ can be determined. Therefore the response vector of the proposed beamformer is given by

$$\mathbf{u} = \pm\left([\hat{u}_1, \hat{u}_2, \cdots, \hat{u}_M]^{\mathrm{T}} + j[\hat{u}_{M+1}, \hat{u}_{M+2}, \cdots, \hat{u}_{2M}]^{\mathrm{T}}\right) \tag{20}$$

where $\pm$ means that if there is a feasible solution to Problem (19), its negative counterpart is also a solution.

This article has been accepted for publication in a future issue of this journal, but has not been fully edited. Content may change prior to final publication. Citation information: DOI 10.1109/TSP.2015.2460221, IEEE Transactions on Signal Processing

IV. Analysis of the Proposed Method

A. Existence of Rank-One Solution

Note that the traditional response vector whose elements are all equal to one is feasible for the constraints in (12). Therefore, the existence of a solution can be confirmed. On the other hand, it is noteworthy that the solution obtained by solving the relaxed SDP problem (16) or (19) may not be exactly rank-one. Nevertheless, the lower the rank of the solution, the better the approximation we would expect. The relationship between the rank of the matrix $\hat{\mathbf{U}}$ and the number of the constraints has been addressed in [37]. It follows from [37] that, for the real-valued problem, the following relationship holds

$$\frac{\mathrm{rank}(\hat{\mathbf{U}})\left(\mathrm{rank}(\hat{\mathbf{U}})+1\right)}{2} \leq M. \tag{21}$$

Therefore, the relaxed SDP problem in (19) is tight for the original QCQP problem with $M \leq 2$. In other words, if the number of constraints is not more than 2, then solving the relaxed SDP problem is equivalent to solving the original QCQP problem. In this case, the principal eigenvector component is exactly the solution to the original problem. Otherwise, the optimal $\hat{\mathbf{u}}$ has to be generated from the general rank solution $\hat{\mathbf{U}}$. For the complex-valued problem, the relationship between the rank of $\mathbf{U}$ and number of constraints has been investigated in [38], which indicates that

$$\mathrm{rank}(\mathbf{U}) \leq \sqrt{M}. \tag{22}$$

In this case, solving the relaxed SDP problem in (16) is equivalent to solving the original QCQP problem when the number of constraints is no more than 3. Moreover, the rank-one solution can be determined by using the well-known rank reduction technique. It follows from [35], [39] that the probability of obtaining a rank-one solution approaches one for the relaxed SDP problem.

Usually, the rank-one approximation is applied by using the eigenvalue-decomposition (EVD).

$$\mathbf{U}^{\#} = \sum_{i=1}^{r} \lambda_i \mathbf{u}_i \mathbf{u}_i^{\mathrm{H}} \tag{23}$$

where $\mathbf{U}^{\#}$ is the solution to the relaxed SDP problem, $r = \mathrm{rank}(\mathbf{U}^{\#})$, $\lambda_1 \geq \lambda_2 \geq \cdots \geq \lambda_r > 0$ are the eigenvalues and $\mathbf{u}_1, \mathbf{u}_2, \cdots, \mathbf{u}_r$ are the corresponding eigenvectors. Thus the suboptimal response vector can be expressed as

$$\hat{\mathbf{u}} = \sqrt{\lambda_1}\mathbf{u}_1. \tag{24}$$

As the probability of obtaining a rank-one solution for the relaxed SDP problem is close to one, (24) provides the optimal response vector with high probability.

An alternative interpretation of the relaxed SDP problem is to solve the QCQP problem in expectation. Consider a stochastic QCQP problem:

$$\begin{aligned} \min_{\mathbf{U}\succeq 0} \quad & E_{\xi\sim N(\mathbf{0},\mathbf{U})}\left\{\xi^{\mathrm{T}}\mathbf{P}\xi^{*}\right\} \\ \text{s.t.} \quad & E_{\xi\sim N(\mathbf{0},\mathbf{U})}\left\{\xi^{\mathrm{H}}\mathbf{B}_m\xi\right\} \geq 1, \quad m = 1, 2, \cdots, M \end{aligned} \tag{25}$$

This article has been accepted for publication in a future issue of this journal, but has not been fully edited. Content may change prior to final publication. Citation information: DOI 10.1109/TSP.2015.2460221, IEEE Transactions on Signal Processing

where we manipulate the statistics of ξ so that the objective function is minimized and the constraints are satisfied in expectation. It is verified that problem (25) is equivalent to problem (16). To obtain the rank-one solution, we carry out the following algorithm:

Input: the relaxed SDP solution $\mathbf{U}^{\#}$ to (16) and the number of randomizations I.

for $i = 1, 2, \cdots, I$

1) generate a random vector $\xi_i \sim N(\mathbf{0}, \mathbf{U}^{\#})$

2) modify ξ_i so that it is feasible for the original QCQP problem, i.e., $\mathbf{u}_i = \frac{\xi_i}{\sqrt{\min_{m=1,2,\cdots,M} \xi_i^{\mathrm{H}} \mathbf{B}_m \xi_i}}$.

end

determine i by $i^{\#} = \arg_{i=1,2,\cdots,I} \min \mathbf{u}_i^{\mathrm{T}} \mathbf{P} \mathbf{u}_i^*$

Output: $\hat{\mathbf{u}} = \mathbf{u}_{i^{\#}}$, which is the approximate solution.

Such a randomized QCQP procedure can be implemented several times to get a better approximation.

Note that the iterative second-order cone programming (SOCP) scheme [40] is also applicable for problem (10) as the magnitude of the response vector can be conservatively approximated by the real part, that is,

$$|u_m| \geq \mathrm{Re}\{u_m\}, \quad m = 1, 2, \cdots, M \tag{26}$$

where $\mathrm{Re}\{\cdot\}$ stands for the real part of its arguments. Thus, the non-convex constraints can be strengthened as

$$\mathrm{Re}\{u_m\} \geq 1, \quad m = 1, 2, \cdots, M. \tag{27}$$

Defining $\mathbf{P} = \mathbf{V}^{\mathrm{H}}\mathbf{V}$, the objective function can be written as

$$\mathbf{u}^{\mathrm{T}} \mathbf{P} \mathbf{u}^* = \|\mathbf{V}\mathbf{u}^*\|^2 \tag{28}$$

Thus, introducing a new scalar non-negative variable τ and a new constraint $\|\mathbf{V}\mathbf{u}^*\| \leq \tau$, problem (10) is converted to

$$\begin{aligned} &\min_{\mathbf{u},\tau} \tau \\ &\text{s.t.} \begin{cases} \|\mathbf{V}\mathbf{u}^*\| \leq \tau \\ \mathrm{Re}\{u_m\} \geq 1, \quad m = 1, 2, \cdots, M \end{cases} \end{aligned} \tag{29}$$

It should be noticed that the feasible set of problem (29) is only a subset of the original problem (10). It follows from [40] that the solution of (29) may not be optimal for (10) and it may turn the original feasible problem into an infeasible one. In this case, the iterative SOCP approach can be performed to obtain the optimal solution [40]. Since the rotation of the adaptive weight by a factor of $\exp(j\phi)$ does not change the output SINR of the beamformer [41], the output SINR of the beamformer remains identical when the response vector is rotated by a factor of $\exp(j\phi)$. In this problem, the rotated angle for the iteration is written as

$$\phi = \angle \left(\sum_{m=1}^{M} u_m \right) \tag{30}$$

This article has been accepted for publication in a future issue of this journal, but has not been fully edited. Content may change prior to final publication. Citation information: DOI 10.1109/TSP.2015.2460221, IEEE Transactions on Signal Processing

where $\angle(\cdot)$ is phase of the arguments. Note that the following inequality holds

$$\begin{aligned}&\sum_{m=1}^{M}\mathrm{Re}\left\{u_m\exp\left(-j\phi\right)\right\}\\&=\mathrm{Re}\left\{\sum_{m=1}^{M}u_m\exp\left(-j\phi\right)\right\}\geq\mathrm{Re}\left\{\sum_{m=1}^{M}u_m\right\}.\end{aligned}\tag{31}$$

For the SDP scheme, the feasible set of problem (16) will always contain the solution of the original problem (10). As the number of constraints is usually small, the relaxed SDP approach is an effective way to approximately solve the problem while the iterative SOCP approach is more beneficial when M is large.

B. Diagonal Loading Analysis

Note that the performance of the proposed RVO-LCMV beamformer may also degrade due to the presence of target at high SNRs. This is because the objective function (9) contains the power of target while the DOA (or DOA and Doppler frequency for STAP) of the target is not included in the constrained points set. To circumvent this problem, a diagonal loading technique is adopted. The corresponding objective function (9) can be rewritten as

$$f(\mathbf{u})=\mathbf{u}^{\mathrm{T}}\left(\mathbf{C}^{\mathrm{H}}\gamma(\hat{\mathbf{R}}+\gamma\mathbf{I})^{-1}\mathbf{C}\right)^{-1}\mathbf{u}^{*}\tag{32}$$

where γ is the diagonal loading factor. Thus, the matrix $\mathbf{P}$ is written as

$$\mathbf{P}=\left(\mathbf{C}^{\mathrm{H}}\gamma(\hat{\mathbf{R}}+\gamma\mathbf{I})^{-1}\mathbf{C}\right)^{-1}=\begin{pmatrix}p_{11}&p_{12}&\cdots&p_{1M}\\p_{21}&p_{22}&\cdots&p_{2M}\\\vdots&\vdots&\ddots&\vdots\\p_{M1}&p_{M2}&\cdots&p_{MM}\end{pmatrix}^{-1}\tag{33}$$

where $p_{\alpha\beta}=\gamma\mathbf{a}_s^{\mathrm{H}}(\theta_\alpha)(\hat{\mathbf{R}}+\gamma\mathbf{I})^{-1}\mathbf{a}_s(\theta_\beta)$ for DBF or $p_{\alpha\beta}=\gamma\mathbf{a}_{s-t}^{\mathrm{H}}(\theta_\alpha,f_{t\alpha})(\hat{\mathbf{R}}+\gamma\mathbf{I})^{-1}\mathbf{a}_{s-t}(\theta_\beta,f_{t\beta})$ for STAP. For DBF implementations, $p_{\alpha\beta}$ can be taken as the output at angle θ_β with adaptive weight $\gamma(\hat{\mathbf{R}}+\gamma\mathbf{I})^{-1}\mathbf{a}_s(\theta_\alpha)$. It can also be taken as the correlation between $\mathbf{a}_s(\theta_\alpha)$ and $\mathbf{a}_s(\theta_\beta)$ which is whitened by the covariance matrix $\hat{\mathbf{R}}+\gamma\mathbf{I}$. Similarly, for the STAP applications, $p_{\alpha\beta}$ can be interpreted as the output at $(\theta_\beta,f_{t\beta})$ with adaptive weight $\gamma(\hat{\mathbf{R}}+\gamma\mathbf{I})^{-1}\mathbf{a}_{s-t}(\theta_\alpha,f_{t\alpha})$ or the whitened correlation between $\mathbf{a}_{s-t}(\theta_\alpha,f_{t\alpha})$ and $\mathbf{a}_{s-t}(\theta_\beta,f_{t\beta})$. Assume that

$$\hat{\mathbf{R}}+\gamma\mathbf{I}=\sum_{q=1}^{Q}\lambda_q\mathbf{v}_q\mathbf{v}_q^{\mathrm{H}}+\sigma^2\sum_{q=Q+1}^{N}\mathbf{v}_q\mathbf{v}_q^{\mathrm{H}}\tag{34}$$

where $\lambda_1\geq\lambda_2\geq\cdots\geq\lambda_Q>\lambda_{Q+1}\approx\lambda_{Q+2}\approx\cdots\approx\lambda_N\approx\sigma^2$ with Q denoting the number of large eigenvalues of matrix $\hat{\mathbf{R}}+\gamma\mathbf{I}$. The first term on the right hand side of (34) corresponds to the signal subspace while the second term is the noise subspace. Thus

$$\begin{aligned}(\hat{\mathbf{R}}+\gamma\mathbf{I})^{-1}&=\sum_{q=1}^{Q}\frac{1}{\lambda_q}\mathbf{v}_q\mathbf{v}_q^{\mathrm{H}}+\frac{1}{\sigma^2}\sum_{q=Q+1}^{N}\mathbf{v}_q\mathbf{v}_q^{\mathrm{H}}\\&=\frac{1}{\sigma^2}\left(\mathbf{I}-\sum_{q=1}^{Q}\frac{\lambda_q-\sigma^2}{\lambda_q}\mathbf{v}_q\mathbf{v}_q^{\mathrm{H}}\right)\end{aligned}\tag{35}$$

This article has been accepted for publication in a future issue of this journal, but has not been fully edited. Content may change prior to final publication. Citation information: DOI 10.1109/TSP.2015.2460221, IEEE Transactions on Signal Processing

It follows from (35) that the elements in $\mathbf{P}$ of (33) corresponding to the DBF and STAP can be written as

$$\begin{aligned} p_{\alpha\beta}^{\text{DBF}} &= \gamma \mathbf{a}_s^{\text{H}}(\theta_\alpha)(\hat{\mathbf{R}}+\gamma\mathbf{I})^{-1}\mathbf{a}_s(\theta_\beta) \\ &= \frac{\gamma}{\sigma^2}\begin{pmatrix} \mathbf{a}_s^{\text{H}}(\theta_\alpha)\mathbf{a}_s(\theta_\beta) \\ -\sum_{q=1}^{Q}\frac{\lambda_q-\sigma^2}{\lambda_q}\mathbf{a}_s^{\text{H}}(\theta_\alpha)\mathbf{v}_q\mathbf{v}_q^{\text{H}}\mathbf{a}_s(\theta_\beta) \end{pmatrix} \end{aligned} \tag{36a}$$

$$\begin{aligned} p_{\alpha\beta}^{\text{STAP}} &= \gamma \mathbf{a}_{s-t}^{\text{H}}(\theta_\alpha, f_{t\alpha})(\hat{\mathbf{R}}+\gamma\mathbf{I})^{-1}\mathbf{a}_{s-t}(\theta_\beta, f_{t\beta}) \\ &= \frac{\gamma}{\sigma^2}\begin{pmatrix} \mathbf{a}_{s-t}^{\text{H}}(\theta_\alpha, f_{t\alpha})\mathbf{a}(\theta_\beta, f_{t\beta}) \\ -\sum_{q=1}^{Q}\frac{\lambda_q-\sigma^2}{\lambda_q}\mathbf{a}_{s-t}^{\text{H}}(\theta_\alpha, f_{t\alpha})\mathbf{v}_q\mathbf{v}_q^{\text{H}}\mathbf{a}(\theta_\beta, f_{t\beta}) \end{pmatrix} \end{aligned} \tag{36b}$$

Generally, the constrained points are around the assumed DOA (or DOA and Doppler for STAP). Therefore, when the target signal is excluded from the training data or the diagonal loading level is higher than the signal power, the second terms of (36a) and (36b) are relatively small for the non-mainlobe directional interference. As the diagonal loading level becomes large, it follows from (36) that

$$\begin{aligned} \lim_{\gamma\to\infty} p_{\alpha\beta}^{\text{DBF}} &= \lim_{\gamma\to\infty} \gamma \mathbf{a}_s^{\text{H}}(\theta_\alpha)(\hat{\mathbf{R}}+\gamma\mathbf{I})^{-1}\mathbf{a}_s(\theta_\beta) \\ &= \lim_{\gamma\to\infty} \frac{\gamma}{\sigma^2}\mathbf{a}_s^{\text{H}}(\theta_\alpha)\mathbf{a}_s(\theta_\beta) \\ &= \mathbf{a}_s^{\text{H}}(\theta_\alpha)\mathbf{a}_s(\theta_\beta) \end{aligned} \tag{37a}$$

$$\begin{aligned} \lim_{\gamma\to\infty} p_{\alpha\beta}^{\text{STAP}} &= \lim_{\gamma\to\infty} \gamma \mathbf{a}_{s-t}^{\text{H}}(\theta_\alpha, f_{t\alpha})(\hat{\mathbf{R}}+\gamma\mathbf{I})^{-1}\mathbf{a}_{s-t}(\theta_\beta, f_{t\beta}) \\ &= \lim_{\gamma\to\infty} \frac{\gamma}{\sigma^2}\mathbf{a}_{s-t}^{\text{H}}(\theta_\alpha, f_{t\alpha})\mathbf{a}_{s-t}(\theta_\beta, f_{t\beta}) \\ &= \mathbf{a}_{s-t}^{\text{H}}(\theta_\alpha, f_{t\alpha})\mathbf{a}_{s-t}(\theta_\beta, f_{t\beta}) \end{aligned} \tag{37b}$$

In this case, the matrix $\mathbf{P}$ is deterministic and thus the optimal response vector can be determined. Equation (37) is preferred when the signal power is unknown.

Note that the mainlobe-to-sidelobe ratio (MSR) of the proposed method can be expressed as

$$\text{MSR} = \frac{\int_{\theta\in\Omega_0}\left|\mathbf{w}^{\text{H}}\mathbf{a}_s(\theta)\right|^2 d\theta}{\int_{\theta\in\Omega,\theta\notin\Omega_0}\left|\mathbf{w}^{\text{H}}\mathbf{a}_s(\theta)\right|^2 d\theta} = \frac{\mathbf{w}^{\text{H}}\mathbf{A}_\theta\mathbf{w}}{\mathbf{w}^{\text{H}}\left(\mathbf{I}-\mathbf{A}_\theta\right)\mathbf{w}} \tag{38}$$

where Ω_0 is the angle sector of mainlobe, Ω is the whole angle range, $\mathbf{I}$ is the identity matrix, and $\mathbf{A}_\theta = \int_{\theta\in\Omega_0}\mathbf{a}_s(\theta)\mathbf{a}_s^{\text{H}}(\theta)d\theta$. In (38), we assume that $\mathbf{C}$ is a proper approximation of the subspace of the mainlobe, i.e., $\mathbf{A}_\theta \approx \mathbf{C}\mathbf{C}^{\text{H}}$. In order to address the sidelobe reduction ability, we consider the noise-limited scenarios where the adaptive weight can be rewritten as $\mathbf{w} = \mathbf{C}\left(\mathbf{C}^{\text{H}}\mathbf{C}\right)^{-1}\mathbf{u}^*$. Thus, it yields

$$\text{MSR} \approx \frac{\|\mathbf{u}\|^2}{\left\|\mathbf{u}^{\text{T}}\left(\mathbf{C}^{\text{H}}\mathbf{C}\right)^{-1}\mathbf{u}^*\right\|^2 - \|\mathbf{u}\|^2} \tag{39}$$

Under the mainlobe constraint, the maximization of (39) is equivalent to

$$\min_{\mathbf{u}} \mathbf{u}^{\text{T}}\left(\mathbf{C}^{\text{H}}\mathbf{C}\right)^{-1}\mathbf{u}^* \quad \text{s.t. } |u_m| \geq 1, \quad m = 1, 2, \cdots, M \tag{40}$$

It follows from (37) that $\lim_{\gamma\to\infty}\mathbf{P} = \left(\mathbf{C}^{\text{H}}\mathbf{C}\right)^{-1}$. Thus, the proposed approach can suppress the sidelobe effectively.

This article has been accepted for publication in a future issue of this journal, but has not been fully edited. Content may change prior to final publication. Citation information: DOI 10.1109/TSP.2015.2460221, IEEE Transactions on Signal Processing

C. Low-Rank Approximation of the Constraint Matrix

In LCMV beamformer, each constraint consumes one DOF. Besides, the more points are imposed, the better mainlobe of the beampattern is maintained. However, if the DOFs of the system are small, the performance degradation due to additional constraints becomes severe because the interference cannot be efficiently suppressed. To circumvent this issue, the low-rank approximation is introduced into the constraints. The rank M_p approximation to $\mathbf{C}$ can be expressed as

$$\mathbf{C} \approx \mathbf{Y}\mathbf{\Sigma}\mathbf{Z}^{\mathrm{H}} \tag{41}$$

where $\mathbf{\Sigma} \in \mathbb{C}^{M_p \times M_p}$ is a diagonal matrix consisting the M_p primary singular values, $\mathbf{Y}$ is the left singular matrix ($\mathbf{Y} \in \mathbb{C}^{N \times M_p}$ for DBF and $\mathbf{Y} \in \mathbb{C}^{NK \times M_p}$ for STAP) and $\mathbf{Z} \in \mathbb{C}^{M \times M_p}$ is the right singular matrix. In the sequel, the reduced rank constraints can be written as $\mathbf{w}^{\mathrm{H}}\mathbf{C} \approx \mathbf{w}^{\mathrm{H}}\mathbf{Y}\mathbf{\Sigma}\mathbf{Z}^{\mathrm{H}} = \mathbf{u}^{\mathrm{T}}$, thus we obtain

$$\mathbf{w}^{\mathrm{H}}\mathbf{Y} = \mathbf{u}^{\mathrm{T}}\mathbf{Z}\mathbf{\Sigma}^{-1} \tag{42}$$

Define $\mathbf{u}_p^{\mathrm{T}} = \mathbf{u}^{\mathrm{T}}\mathbf{Z}\mathbf{\Sigma}^{-1}$ which is small in dimension, then the adaptive weight can be computed as

$$\mathbf{w} = \hat{\mathbf{R}}^{-1}\mathbf{Y}(\mathbf{Y}^{\mathrm{H}}\hat{\mathbf{R}}^{-1}\mathbf{Y})^{-1}\mathbf{u}_p^{*} \tag{43}$$

Thus, the problem in (12) can be expressed as

$$\begin{aligned} &\min_{\mathbf{u}_p} \mathbf{u}_p^{\mathrm{T}}(\mathbf{Y}^{\mathrm{H}}\hat{\mathbf{R}}^{-1}\mathbf{Y})^{-1}\mathbf{u}_p^{*} \\ &\text{s.t. } \mathbf{u}_p^{\mathrm{H}}\mathbf{B}_m\mathbf{u}_p \geq 1,\ m = 1, 2, \cdots, M_p. \end{aligned} \tag{44}$$

D. Computational Complexity Analysis

Note that the proposed approach does not provide a closed-form solution and the optimal response vector must be obtained using numerical method. A common way to solve the relaxed SDP problem is to use the interior-point method which is able to provide precise solution. The computational complexity is provably polynomial in the problem size.

In particular, by introducing Lagrange multipliers $\rho = [\rho_1, \cdots, \rho_M]^{\mathrm{T}} \in \mathbb{R}_+^M$ for the inequality constraints, we obtain

$$\begin{aligned} g(\mathbf{U}, \rho) &= \min_{\mathbf{U} \succeq 0, \rho_m \geq 0} \mathrm{tr}\left\{\mathbf{P}\mathbf{U}\right\} + \sum_{m=1}^{M} \rho_m \left(\mathrm{tr}\left\{\mathbf{B}_m\mathbf{U}\right\} - 1\right) \\ &= \min_{\mathbf{U} \succeq 0, \rho_m \geq 0} \mathrm{tr}\left\{\left(\mathbf{P} + \sum_{m=1}^{M} \rho_m\mathbf{B}_m\right)\mathbf{U}\right\} - \sum_{m=1}^{M} \rho_m \end{aligned} \tag{45}$$

It follows from [42], [43] that the minimization over $\mathbf{U}$ is bounded only if

$$\mathbf{P} + \sum_{m=1}^{M} \rho_m\mathbf{B}_m \succeq 0 \tag{46}$$

This article has been accepted for publication in a future issue of this journal, but has not been fully edited. Content may change prior to final publication. Citation information: DOI 10.1109/TSP.2015.2460221, IEEE Transactions on Signal Processing

Thus, we obtain the dual problem of the SDP problem as

$$\begin{aligned} &\max_{\rho} -\rho^{\mathrm{T}}\mathbf{1}_M \\ &\text{s.t.} \quad \begin{cases} \mathbf{P} + \sum_{m=1}^{M} \rho_m \mathbf{B}_m \succeq 0 \\ \rho_m \geq 0 \end{cases} \end{aligned} \tag{47}$$

where $\mathbf{1}_M$ is an $M \times 1$ vector with all its elements are equal to one. It has been shown in [42], [43] that the dual problem in (47) can be solved efficiently with the worst-case complexity of $\mathcal{O}\left(M^{4.5}\right)$. This complexity does not assume sparsity or any special structures in the data matrices $\mathbf{P}, \mathbf{B}_1, \cdots, \mathbf{B}_M$. Note that the matrices $\mathbf{B}_1, \cdots, \mathbf{B}_M$ are sparse. A custom-built interior-point algorithm can solve the problem with a worst-case complexity of $\mathcal{O}\left(M^{3.5}\right)$ by exploiting the sparsity of matrices $\mathbf{B}_1, \cdots, \mathbf{B}_M$ [43].

Note that the number of constraints M is usually a small scale. Compared with the state-of-the-art techniques which calculate the adaptive weight vector directly [8]–[10], [31] or calculate the adaptive weight matrix [29], [30], the computational complexity of the proposed method is reduced considerably.

In STAP applications, the length of the weight is NK which is a great number in practice. Thus the computational load is huge for the state-of-the-art robust STAP implementations [8]–[10], [26]–[31]. In contrast, the proposed method tries to determine the optimal response vector whose size is much smaller than that of the adaptive weight. For instance, the number of constraints are set as $M_1 = 3$ in spatial domain and $M_2 = 3$ in temporal domain. Note that the number of constraints is independent on the length of the adaptive weight in the proposed approach. Moreover, STAP radar searches all K Doppler channels to detect the possible target. Thus, problem in (16) needs to be solved for K times, which induces a complexity of $\mathcal{O}\left(M^{3.5}K\right)$. Besides, the SMI technique is required as shown in (8), which is solved in a complexity of $\mathcal{O}\left(N^2K^2\right)$ by using reweighted least squares (RLS) to update the covariance matrix. Thus, the overall complexity of the proposed method in STAP is

$$\mathcal{O}\left(M^{3.5}K\right) + \mathcal{O}\left(N^2K^2\right) \tag{48}$$

Since M is much smaller than N and K, the computational complexity for optimally determining the response vector is negligible compared with that of the SMI technique. In contrast, techniques that directly calculate the adaptive weight vector have a complexity of $\mathcal{O}\left(N^3K^3K\right) = \mathcal{O}\left(N^3K^4\right)$, while techniques that calculate the adaptive weight matrix have a complexity of $\mathcal{O}\left(N^{4.5}K^{4.5}K\right) = \mathcal{O}\left(N^{4.5}K^{5.5}\right)$. Thus, the proposed method is superior to the state-of-the-art techniques in computational complexity.

V. Simulation Results

In this section, Monte Carlo simulation is carried out to evaluate the performance of the proposed method. The simulation results for the DBF are presented in the first and second subsections while those for the STAP are presented in the following three subsections. Table I and II provide the parameters which are used to reproduce the simulation results in this paper. Note that the training samples are probably corrupted by the target signal. Moreover, the target probably occupies several range bins, especially in the scenarios where the high resolution radar needs to handle multiple targets. In the simulation examples, we assume that 5 snapshots are corrupted by the target signal.

This article has been accepted for publication in a future issue of this journal, but has not been fully edited. Content may change prior to final publication. Citation information: DOI 10.1109/TSP.2015.2460221, IEEE Transactions on Signal Processing

TABLE I: Parameters for DBF

Parameter	Value	Parameter	Value
Carrier wavelength	0.03m	Number of elements	10
Element spacing	0.015m	Number of snapshots	200
Mainlobe direction	0°	Interference DOA	30°
Actual target DOA	2°	Interference-to-noise ratio	30dB
SNR	10dB		

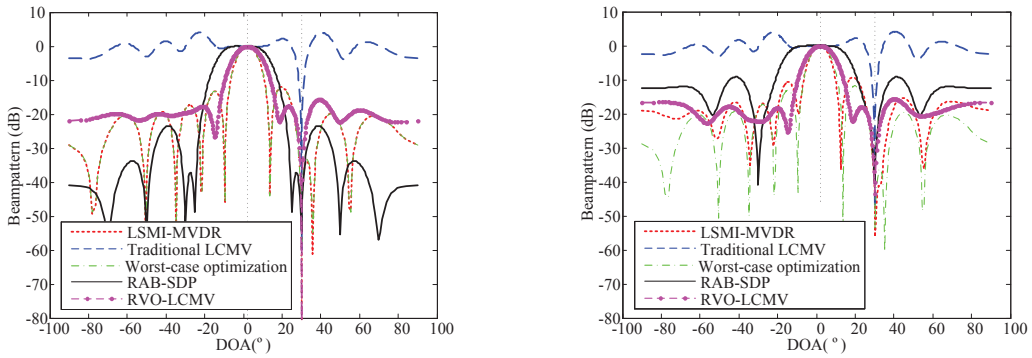

Fig. 2: Beampatterns of various approaches. (a) Theoretical covariance matrix. (b) Estimated covariance matrix.

A. Beampattern Comparison for DBF

In this experiment, we examine the performance of the proposed RVO-LCMV approach in the DBF radar. For comparison, the simulation results of the LSMI-MVDR beamformer, traditional LCMV beamformer, worst-case optimization beamformer [8] and SDP based robust adaptive beamformer (namely, the RAB-SDP in [29]) are presented as well.

Assume the accurate DOA of the target is known to the radar receiver in this example. The true and estimated covariance matrices are adopted in Figs. 2(a) and (b), respectively. The constrained beamwidth of the mainlobe is 6° for the traditional LCMV, RAB-SDP [29] and proposed beamformers. The ripple of the RAB-SDP approach is set as 0.3dB. The constrained points are at angles -3°, -1°, 0°, 1° and 3°. Because the accurate target DOA is known, the mainlobes of all the beamformers are well maintained. It is seen that the sidelobes of all these beamformers (except the traditional LCMV beamformer) are very low in the case of theoretical covariance matrix. For the estimated covariance matrix, however, the sidelobe of the proposed beamformer is much lower than those of other methods. Besides, the mainlobe of the proposed method is well maintained. Thus, the robustness of the proposed RVO-LCMV beamformer is considerably enhanced.

In practice, the exact knowledge of target parameters is unknown to the receiver. Instead, their estimates are usually adopted, especially in target tracking or confirmation situations. In this experiment, the mismatched target

This article has been accepted for publication in a future issue of this journal, but has not been fully edited. Content may change prior to final publication. Citation information: DOI 10.1109/TSP.2015.2460221, IEEE Transactions on Signal Processing

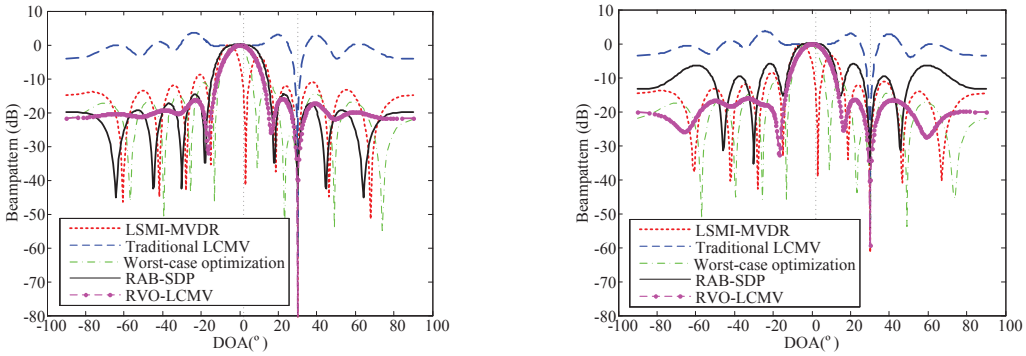

Fig. 3: Beampatterns of various approaches. (a) Theoretical covariance matrix. (b) Estimated covariance matrix.

DOA is utilized. In particular, the actual DOA of the target is 2° while the constrained angles are -3°, -1°, 0°, 1°, and 3°. The theoretical and estimated covariance matrices are used in Figs. 3(a) and (b), respectively. Because of the mismatch between the assumed and actual DOAs of the target, LSMI-MVDR beamformer misinterprets the target as interference and tries to suppress it, thus causing target self-nulling and severe performance degradation. All other methods are robust against the presence of the target. The worst-case optimization beamformer belongs to the diagonal loading robust approach with the diagonal loading factor optimally calculated, thus avoiding the self-nulling phenomenon. It should be noted that, though the traditional LCMV beamformer is robust against DOA errors, its sidelobe is very high and its mainlobe is distorted. For the estimated covariance matrix in Fig. 3(b), it is seen that the proposed method outperforms the other methods in terms of lower sidelobe.

In Fig. 4, the rank-one approximations of the response vectors generated by the EVD and randomization methods are plotted. The response vector of the traditional LCMV beamformer is also presented for comparison. Since the response vector of the traditional LCMV beamformer is an all-one vector, all its elements overlap. In contrast, the elements of the response vector of the proposed RVO-LCMV method are complex-valued. It is seen that the two optimal response vectors generated by EVD and randomization methods are different in phase.

B. Output SINR Performance

In this experiment, the output SINR performance is evaluated for the methods aforementioned. Note that the training data is corrupted by the target and the assumed DOA of target is mismatched with the actual DOA. Figs. 5(a) and (b) show the output SINR with respect to input SNR and number of snapshots, respectively. The optimal SINR performance is provided for comparison. It is observed in Fig. 5 that the LSMI-MVDR beamformer is sensitive to input SNR and the performance degrades at high SNRs. The worst-case optimization, RAB-SDP, traditional LCMV, and proposed RVO-LCMV beamformers are robust against input SNR. Moreover, the proposed method provides substantial performance improvement compared with the traditional LCMV beamformer which degrades severely in performance due to the high sidelobe and distorted mainlobe. The performance of the LSMI-MVDR

This article has been accepted for publication in a future issue of this journal, but has not been fully edited. Content may change prior to final publication. Citation information: DOI 10.1109/TSP.2015.2460221, IEEE Transactions on Signal Processing

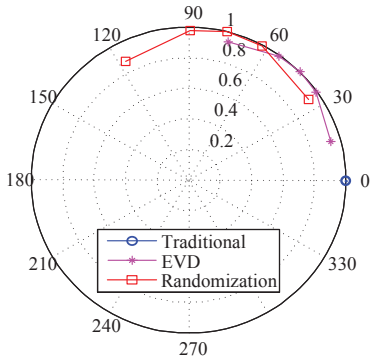

Fig. 4: Magnitude and phase of the response vector.

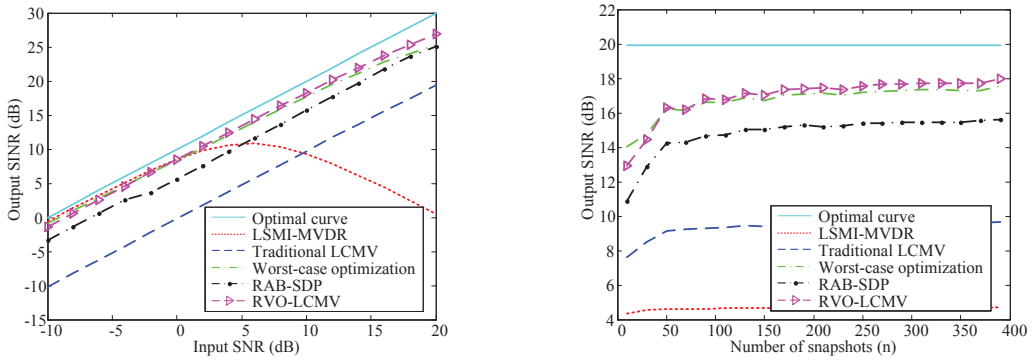

(a) (b)

Fig. 5: Performance comparison of output SINR. (a) Output SINR versus input SNR. (b) Output SINR versus number of snapshots.

beamformer is even worse because of the target self-nulling. In contrast, the worst-case optimization, RAB-SDP, and proposed RVO-LCMV beamformers can maintain their performance for small samples. Furthermore, the proposed LCMV-RVO performs the best.

Fig. 6 plots the output SINRs of the aforementioned beamformers for different DOA errors. It is clearly seen that even small DOA error can lead to severe performance degradation for the LSMI-MVDR beamformer. However, other approaches are more robust against the DOA error. Note that the worst-case optimization beamformer is only robust for a limited region. That is, its performance degrades dramatically when the DOA error is much larger. Although the traditional LCMV beamformer is robust over $[-5^\circ, 5^\circ]$, its output SINR is much lower than that of the proposed RVO-LCMV method. The performance of the RAB-SDP beamformer is a little bit worse than that of the proposed RVO-LCMV beamformer over $[-5^\circ, 5^\circ]$. It has been pointed out in [29] that the robust response region of the RAB-SDP beamformer can be flexibly controlled with specified beamwidth and response ripple. Therefore, it can be robust over a large DOA error range. In a word, the proposed RVO-LCMV beamformer performs almost

This article has been accepted for publication in a future issue of this journal, but has not been fully edited. Content may change prior to final publication. Citation information: DOI 10.1109/TSP.2015.2460221, IEEE Transactions on Signal Processing

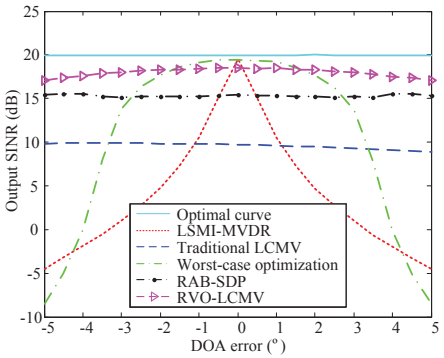

Fig. 6: Output SINR versus DOA error.

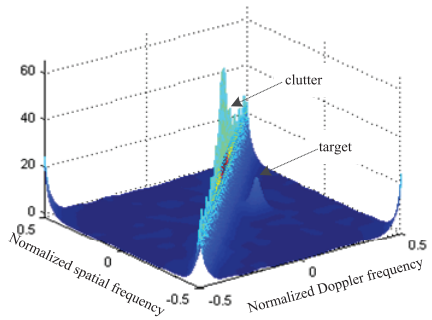

Fig. 7: Capon spectrum of clutter and target.

the best in the whole tested DOA error range, and its maximum performance loss is less than 4dB when the DOA error is smaller than 5°.

In the following three subsections, experimental simulations have been carried out to evaluate the effectiveness of the proposed RVO-LCMV method in STAP applications. Without loss of generality, the sidelooking geometry is utilized [1]. Fig. 7 shows the Capon spectral estimation, which is calculated by

$$z(f_s, f_t) = \frac{1}{\mathbf{a}_{s-t}^{\mathrm{H}}(f_s, f_t)\hat{\mathbf{R}}^{-1}\mathbf{a}_{s-t}(f_s, f_t)} \tag{49}$$

where $\mathbf{a}_{s-t}(f_s, f_t) = \mathbf{a}_t(f_t) \otimes \mathbf{a}_s(f_s)$ with f_t and f_s being the normalized Doppler frequency and normalized spatial frequency, respectively. It is seen that the clutter is coupled in spatial and temporal domains, and its clutter ridge is diagonally distributed in the sidelooking geometry of STAP radar. The target is assumed in the range bins 148 to 152 and all snapshots are used as training data. The other simulation parameters are listed in Table II for the STAP implementations.

C. Beampattern Comparison for STAP

Fig. 8 shows the space-time beampatterns of the LSMI-MVDR, traditional LCMV, worst-case optimization, RAB-SDP, and proposed RVO-LCMV methods. The pentagrams in these figures stand for the true target position. Note

This article has been accepted for publication in a future issue of this journal, but has not been fully edited. Content may change prior to final publication. Citation information: DOI 10.1109/TSP.2015.2460221, IEEE Transactions on Signal Processing

TABLE II: Parameters for STAP

Parameter	Value	Parameter	Value
Carrier wavelength	0.32m	Number of elements	10
Element spacing	0.16m	Number of pulses	10
Pulse repetitive frequency	2000Hz	Number of ranges	300
Platform velocity	160m/s	Clutter-to-noise ratio	50dB
Platform height	6000m	SNR	20dB
Mainlobe direction	0°	Actual target direction	2°
Assumed target velocity	50m/s	Actual target velocity	52m/s

that Figs. 8(d) and (e) depict the space-time beampatterns of the RAB-SDP method. In Fig. 8(d), the adaptive weight vector is adopted which is obtained by spectrum factorization, while in Fig. 8(e), the adaptive weight matrix is utilized to calculate the space-time beampattern. It is seen that the rank-one weight vector derived by the spectrum factorization is invalid while the weight matrix determined by SDP approach works well. As shown in Fig. 8, the mainlobe of LSMI-MVDR method is distorted due the presence of target in the training data. The space-time beampattern of the traditional LCMV method is also distorted and its mainlobe is lower than its sidelobe, which causes a high false alarm probability especially in non-stationary environments. It should be noted that the space-time beampattern of the worst-case optimization method also suffers from distortion for high SNRs. It is seen in Fig. 8(c) that the target point is close to the notch of the beampattern, which indicates a mismatch between the mainlobe and the true target. In contrast, the proposed RVO-LCMV method outperforms other methods in terms of both lower sidelobe and better-maintained mainlobe of the space-time beampattern.

Figs. 9-10 show the magnitude and phase contour map of the response vector of the proposed RVO-LCMV method in STAP radar. Both the EVD and randomization methods are evaluated in the procedure of rank-one approximation. Nine constrained points surrounding the assumed target are chosen. The constrained spatial and Doppler frequencies are $f_{sc} = f_{s0} + \frac{1}{2N}[-1, 0, 1]^{\mathrm{T}}$ and $f_{tc} = f_{t0} + \frac{1}{2K}[-1, 0, 1]^{\mathrm{T}}$, respectively, where f_{s0} and f_{t0} denote the assumed spatial and Doppler frequencies corresponding to the pointing direction of antenna and assumed target velocity, respectively. It is seen that the contour map of the response vector approximates an inclined plane.

D. Output SCNR Performance

The output signal-to-clutter-plus-noise ratio (SCNR) curves versus input SNR and number of snapshots are shown in Figs. 11(a) and (b), respectively. The optimal curve is also depicted in Fig. 11 for comparison. It is seen that the LSMI-MVDR method is sensitive to input SNR especially at high SNRs. The performance degradation of the traditional LCMV method is evident compared with other methods. However, the worst-case optimization, RAB-SDP (using weight matrix) and proposed RVO-LCMV methods are all robust against input SNR and number of snapshots in the STAP applications. Moreover, the proposed method outperforms other methods in terms of output SCNR and convergence rate. It should be noticed that the computational load of the RAB-SDP method is extremely heavy because the dimension of the weight matrix is $NK \times NK = 10000$, while the dimension of matrix $\mathbf{U}$ in

This article has been accepted for publication in a future issue of this journal, but has not been fully edited. Content may change prior to final publication. Citation information: DOI 10.1109/TSP.2015.2460221, IEEE Transactions on Signal Processing

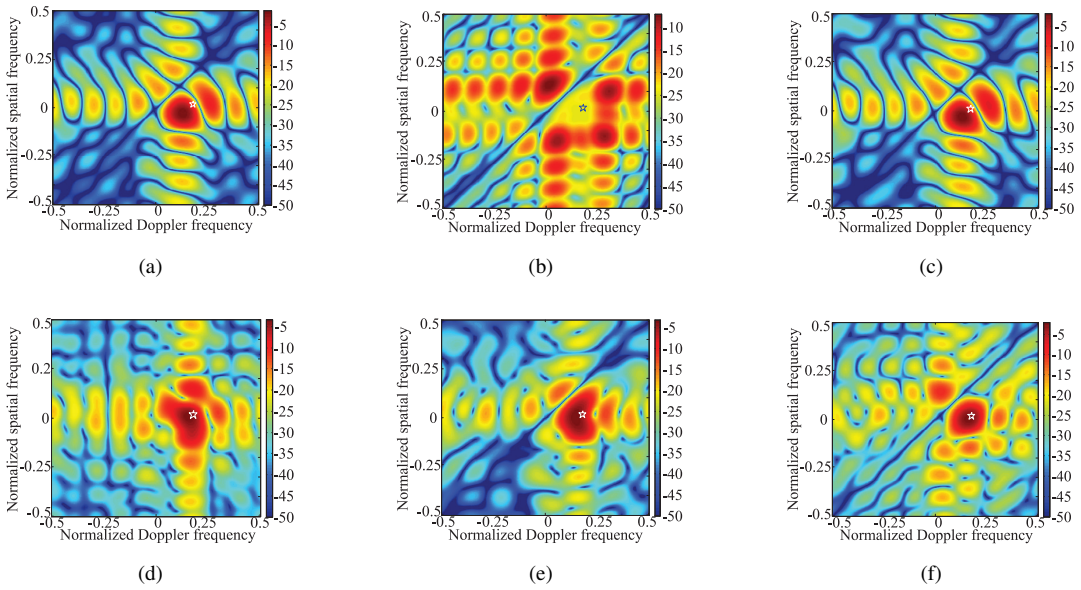

Fig. 8: Space-time beampatterns of various approaches. (a) LSMI-MVDR method. (b) Traditional LCMV method. (c) Worst-case optimization method. (d) RAB-SDP method using weight vector. (e) RAB-SDP method using weight matrix. (f) Proposed RVO-LCMV method.

Fig. 9: Magnitude of the response vector. (a) EVD method. (b) Randomization method.

Fig. 10: Phase of the response vector. (a) EVD method. (b) Randomization method.

This article has been accepted for publication in a future issue of this journal, but has not been fully edited. Content may change prior to final publication. Citation information: DOI 10.1109/TSP.2015.2460221, IEEE Transactions on Signal Processing

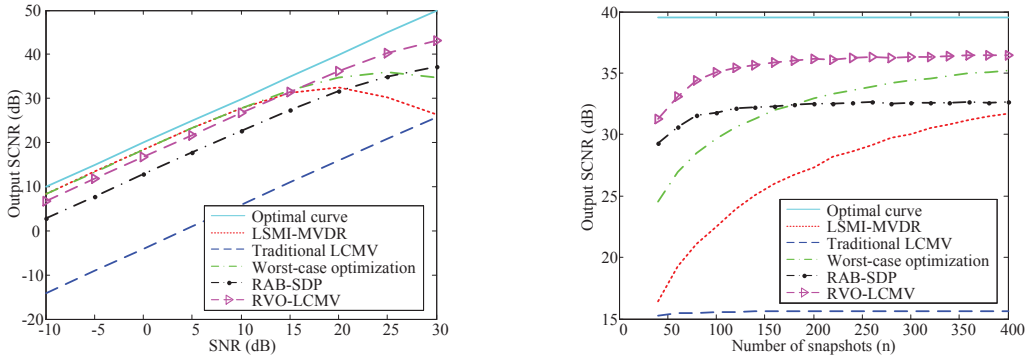

Fig. 11: Comparison of output SCNR performance. (a) Output SCNR versus input SNR. (b) Output SCNR versus number of snapshots.

the proposed approach is relatively small, which only takes $9 \times 9 = 81$ in this example.

In Fig. 12, we evaluate the DOA and Doppler frequency error tolerance of the LSMI-MVDR, traditional LCMV, worst-case optimization, RAB-SDP using weight vector, RAB-SDP using weight matrix and proposed RVO-LCMV methods. It is seen that the performance degradation of the traditional LCMV method is substantial. Meanwhile, the LSMI-MVDR method has a limited robust region due to its performance degradation at high SNRs. The worst-case optimization method is robust against DOA and Doppler frequency errors and provides the moderate performance. The performance of the RAB-SDP method using weight vector is even worse than that of the traditional LCMV method. However, the RAB-SDP method using weight matrix performs well. It is also seen that the proposed RVO-LCMV method outperforms other methods with a wider robust region in DOA and Doppler frequency error range.

E. SCNR loss Performance

In this subsection, the SCNR loss with respect to the normalized Doppler frequency is tested. The SCNR loss is defined as the ratio of clutter-limited output SCNR to noise-limited output SNR, that is,

$$\text{SCNR}_{\text{loss}} = \frac{\text{SCNR}_{\text{out}}}{\text{SNR}_{\text{out}}} = \frac{\mathbf{w}^{\text{H}}\mathbf{R_s}\mathbf{w}}{\mathbf{w}^{\text{H}}\mathbf{R_{cn}}\mathbf{w}} \frac{\sigma_n^2}{\sigma_s^2 NK} \tag{50}$$

where $\mathbf{R_s}$ and $\mathbf{R_{cn}}$ are respectively the target covariance matrix and clutter-plus-noise covariance matrix, σ_s^2 and σ_n^2 are the powers of target and white Gaussian noise.

The SCNR loss curves are plotted in Fig. 13 for the LSMI-MVDR, traditional LCMV, worst-case optimization, RAB-SDP (using weight matrix), and proposed RVO-LCMV methods. For comparison, the optimal curve is provided as well. The contaminated training data and inaccurate target parameters are used in this simulation. As shown in Fig. 13, the performance improvement of the proposed RVO-LCMV method is substantial compared with other methods when the Doppler frequencies are large. However, the performance of the proposed method degrades at

This article has been accepted for publication in a future issue of this journal, but has not been fully edited. Content may change prior to final publication. Citation information: DOI 10.1109/TSP.2015.2460221, IEEE Transactions on Signal Processing

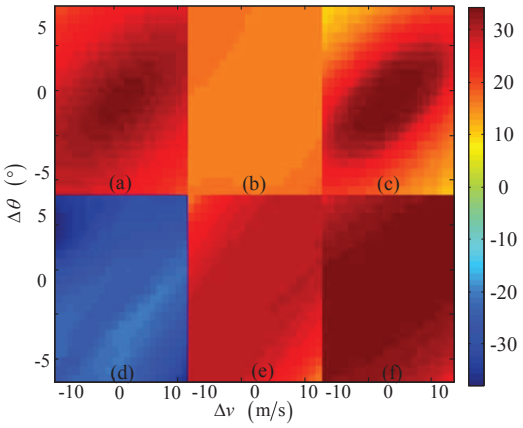

Fig. 12: Output SCNR versus angle and Doppler frequency errors. (a) LSMI-MVDR method. (b) Traditional LCMV method. (c) Worst-case optimization method. (d) RAB-SDP using weight vector. (e) RAB-SDP method using weight matrix. (f) Proposed RVO-LCMV method.

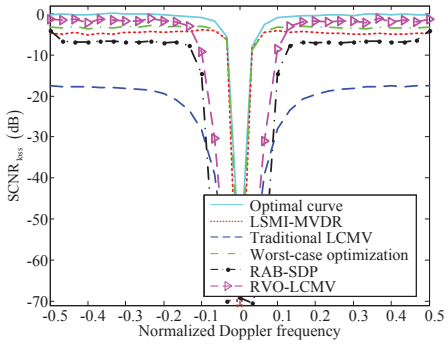

Fig. 13: SCNR loss versus normalized Doppler frequency.

small Doppler frequencies. Indeed, when the assumed Doppler frequency of target is close to the clutter ridge, the minimization of the output covariance will conflict with the constraints. Thus, the traditional LCMV, RAB-SDP and proposed methods degrade in SCNR loss performance at small Doppler frequencies. However, it is seen that the worst-case optimization method can maintain its performance at small Doppler frequencies. The wide notch in the SCNR loss of the proposed method is the cost for robustness, which results in a thicker region in the angle/Doppler plane around the clutter ridge where detection is non-viable. This drawback occurs every time a robust implementation of STAP is applied [33]. A trade-off has to be always found between robustness and target detection capability close to the clutter ridge.

VI. Conclusion

The traditional LCMV beamformer suffers high sidelobe and distorted mainlobe of the beampattern, which causes severe performance degradation. In this paper, we have devised a robust variant of the LCMV beamformer based on

response vector optimization. The proposed method is firstly formulated as a non-convex QCQP problem, and then transformed into a SDP problem. By using the diagonal loading technique, the proposed approach enjoys lower sidelobe and well-maintained mainlobe of the beampattern. The performance improvement is substantial for both DBF and STAP. Moreover, the devised algorithm has a much wider robust region of DOA and/or Doppler frequency errors. Furthermore, the computational complexity of the proposed method is considerably reduced compared with the state-of-the-art techniques.

REFERENCES

[1] J. R. Guerci, *Space-Time Adaptive Processing for Radar*. Norwood, MA: Artech, House, 2003.

[2] J. Capon, "High-resolution frequency wavenumber spectrum analysis," *Proc. of the IEEE*, vol. 57, no. 8, pp. 1408-1418, Aug. 1969.

[3] W. L. Melvin and M. E. Davis, "Adaptive cancellation method for geometry-induced non-stationary bistatic clutter environments," *IEEE Trans. Aerosp. Electron. Syst.*, vol. 43, no. 2, pp. 651-672, Apr. 2007.

[4] C. T. Capraro, G. T. Capraro, I. Bradaric, D. D. Weiner, M. C. Wicks, and W. J. Baldygo, "Implementing digital terrain data in knowledge-aided space-time adaptive processing," *IEEE Trans. Aerosp. Electron. Syst.*, vol. 42, no. 3, pp. 1080-1099, Jul. 2006.

[5] B. D. Carlson, "Covariance matrix estimation errors and diagonal loading in adaptive arrays," *IEEE Trans. Aerosp. Electron. Syst.*, vol. 24, no. 4, pp. 397-401, Jul. 1988.

[6] H. Cox, R. M. Zeskind, and M. M. Owen, "Robust adaptive beamforming," *IEEE Trans. Acoust. Speech, Signal Process.*, vol. 35, no. 10, pp. 1365-1376, Oct. 1987.

[7] R. Wu, Z. Bao, and Y. Ma, "Control of peak sidelobe level in adaptive arrays," *IEEE Trans. Antennas Propag.*, vol. 44, no. 10, pp. 1341-1347, Oct. 1996.

[8] S. A. Vorobyov, A. B. Gershman, and Z. Q. Luo, "Robust adaptive beamforming using worst-case performance optimization: A solution to the signal mismatch problem," *IEEE Trans. Signal Process.*, vol. 51, no. 2, pp. 313-324, Feb. 2003.

[9] J. Li, P. Stoica, and Z. Wang, "On robust Capon beamforming and diagonal loading," *IEEE Trans. Signal Process.*, vol. 51, no. 7, pp. 1702-1715, Jul. 2003.

[10] R. G. Lorenz and S. P. Boyd, "Robust minimum variance beamforming," *IEEE Trans. Signal Process.*, vol. 53, no. 5, pp. 1684-1696, May 2005.

[11] J. Li, P. Stoica, and Z.Wang, "Doubly constrained robust Capon beamformer," *IEEE Trans. Signal Process.*, vol. 52, no. 9, pp. 2407-2423, Sep. 2004.

[12] A. Beck and Y. C. Eldar, "Doubly constrained robust Capon beamformer with ellipsoidal uncertainty sets," *IEEE Trans. Signal Process.*, vol. 55, no. 2, pp. 753-758, Feb. 2007.

[13] S. A. Vorobyov, H. Chen, and A. B. Gershman, "On the relationship between robust minimum variance beamformers with probabilistic and worst-case distrortionless response constraints," *IEEE Trans. Signal Process.*, vol. 56, no. 11, pp. 5719-5724, Nov. 2008.

[14] A. Hassanien, S. A. Vorobyov, and K. M. Wong, "Robust adaptive beamforming using sequential programming: An iterative solution to the mismatch problem," *IEEE Signal Process. Lett.*, vol. 15, pp. 733-736, Nov. 2008.

[15] D. D. Feldman and L. J. Griffiths, "A projection approach to robust adaptive beamforming," *IEEE Trans. Signal Process.*, vol. 42, no. 4, pp. 867-876, Apr. 1994.

[16] L. Chang and C. C. Yeh, "Performance of DMI and eigenspace-based beamformers," *IEEE Trans. Antennas Propag.*, vol. 40, no. 11, pp. 1336-1347, Nov. 1992.

[17] M. Wax and T. Kailath, "Detection of signals by information theoretic criteria," *IEEE Trans. Acoust., Speech, Signal Process.*, vol. 33, no. 2, pp. 387-392, Apr. 1985.

[18] L. Huang, S. Wu, and X. Li, "Reduced-rank MDL method for source enumeration in high-resolution array processing," *IEEE Trans. Signal Process.*, vol. 55, no. 12, pp. 5658-5667, Dec. 2007.

[19] L. Huang and H. C. So, "Source enumeration via MDL criterion based on linear shrinkage estimation of noise subspace covariance matrix," *IEEE Trans. Signal Process.*, vol. 61, no. 19, pp. 4806-4821, Oct. 2013.

[20] O. L. Forst, "An algorithm for linearly constrained adaptive processing," *Proc. of the IEEE*, vol. 60, no. 8, pp. 926-935, Aug. 1972.

[21] K. Takao, H. Fujita, and T. Nishi, "An adaptive array under directional constraint," *IEEE Trans. Antennas Propag.*, vol. 24, no. 5, pp. 662-669, Sep. 1976.

[22] S. P. Applebaum and D. J. Chapman, "Adaptive arrays with main beam constraints," *IEEE Trans. Antennas Propag.*, vol. AP-24, no. 5, pp. 650-662, Sep. 1976.

[23] M. H. Er and A. Cantoni, "Derivative constraints for broad-band element space antenna array processors," *IEEE Trans Acoust., Speech, Signal Process.*, vol. 31, no. 6, pp. 1378-1393, Dec. 1983.

[24] C. Y. Tseng and L. J. Griffiths, "A unified approach to the design of linear constraints in minimum variance adaptive beamformers," *IEEE Trans. Antennas Propag.*, vol. 40, no. 12, pp. 1533-1542, Dec. 1992.

[25] J. W. Xu, G. S. Liao, and S. Q. Zhu, "Robust LCMV beamforming based on phase response constraint," *Electron. Lett.*, vol. 48, no. 20, pp. 1304-1306, Sep. 2012.

[26] S. D. Somasundaram, "Linearly constrained robust Capon beamforming," *IEEE Trans. Signal Process.*, vol. 60, no. 11, pp. 5845-5856, Nov. 2012.

[27] C. Y. Chen and P. P. Vaidyanathan, "Quadratically constrained beamforming robust against direction-of-arrival mismatch," *IEEE Trans. Signal Process.*, vol. 55, no. 8, pp. 4139-4150, Aug. 2007.

[28] Z. L. Yu, W. Ser, M. H. Er, Z. H. Gu, and Y. Q. Li, "Robust adaptive beamformers based on worst-case optimization and constraints on magnitude response," *IEEE Trans. Signal Process.*, vol. 57, no. 7, pp. 2615-2628, Jul. 2009.

[29] Z. L. Yu, M. H. Er, and W. Ser, "A novel adaptive beamformer based on semidefinite programming (SDP) with constraints on magnitude response," *IEEE Trans. Antennas Propag.*, vol. 56, no. 5, pp. 1297-1307, May 2008.

[30] Z. L. Yu, Z. H. Gu, J. J. Zhou, Y. Q. Li, W. Ser, and M. H. Er, "A robust adaptive beamformer based on worst-case semi-definite programming," *IEEE Trans. Signal Process.*, vol. 58, no. 11, pp. 5914-5919, Nov. 2010.

[31] D. J. Xu, R. He, and F. Shen, "Robust beamforming with magnitude response constraints and conjugate symmetric constraint," *IEEE Commun. Lett.*, vol. 17, no. 3, pp.561-564, Mar. 2013.

[32] J. R. Guerci, "Theory and application of covariance matrix tapers for robust adaptive beamforming," *IEEE Trans. Signal Process.*, vol. 47, no. 4, pp. 977-985, Apr. 1999.

[33] D. Cristallini and W. Bürger, "A robust direct data domain approach for STAP," *IEEE Trans. Signal Process.*, vol. 60, no. 3, pp. 1283-1294, Mar. 2012.

[34] I. S. Reed, J. D. Mallett, and L. E. Brennan, "Rapid convergence rate in adaptive arrays," *IEEE Trans. Aerosp. Electron. Syst.*, vol. AES-10, no. 6, pp. 853-863, Nov. 1974.

[35] Z. Q. Luo, W. K. Ma, A. M. So, Y. Y. Ye, and S. Z. Zhang, "Semidefinite relaxation of quadratic optimization problems," *IEEE Signal Process. Mag.*, vol. 27, no. 3, pp. 20-34, May 2010.

[36] S. Boyd and L. Vandenberghe. *Convex Optimization*. Cambridge, U.K.: Cambridge Univ. Press, 2004.

[37] G. Pataki, "On the rank of extreme matrices in semidefinite programs and the multiplicity of optimal eigenvalues," *Math. Oper. Res.*, vol. 23, no. 2, pp. 339-358, May 1998.

[38] Y. Huang and D. P. Palomar, "Rank-constrained separable semidefinite programming with applications to optimal beamforming," *IEEE Trans. Signal Process.*, vol. 58, no. 2, pp. 664-678, Feb. 2010.

[39] A. Khabbazibasmenj, S. A. Vorobyov, and A. Hassanien, "Robust adaptive beamforming based on steering vector estimation with as little as possible prior information," *IEEE Trans. Signal Process.*, vol. 60, no. 6, pp. 2974-2987, Jun. 2012.

[40] N. Bornhorst, M. Pesavento, and A. B. Gershman, "Distributed beamforming for multi-group multicasting relay networks," *IEEE Trans. Signal Process.*, vol. 60, no. 1, pp. 221-232, Jan. 2012.

[41] Y. C. Eldar, A. Nehorai, and P. S. Rosa, "A competitive mean-squared error approach to beamforming," *IEEE Trans. Signal Process.*, vol. 55, no. 11, pp. 5143-5154, Nov. 2007.

[42] L. Vandenberghe and S. Boyd, "Semidefinite programming," *SIAM Rev.*, vol. 38, pp. 49-95, Mar. 1996.

[43] C. Helmberg, F. Rendl, R. Vanderbei, and H. Wolkowicz, "An interior-point method for semidefinite programming," *SIAM J. Optim.*, vol. 6, no. 2, pp. 342-361, 1996.

This article has been accepted for publication in a future issue of this journal, but has not been fully edited. Content may change prior to final publication. Citation information: DOI 10.1109/TSP.2015.2460221, IEEE Transactions on Signal Processing

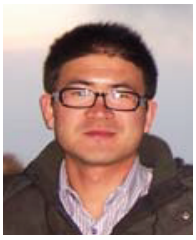

Jingwei Xu was born in Shandong. He received the B.S. degree in electrical engineering from Xidian University, Xian, China, in 2010. He is currently working toward the Ph.D. degree in the National Key Laboratory of Radar Signal Processing, Xidian University.

His research interests include frequency diverse array, MIMO radar signal processing, robust adaptive beamforming and space-time adaptive processing.

Guisheng Liao (M'96) was born in Guangxi. He received the B.S. degree from Guangxi University, Guangxi, China, and the M.S. and Ph.D. degrees from Xidian University, Xian, China, in 1985, 1990, and 1992, respectively.

He is currently a Professor at the National Laboratory of Radar Signal Processing, Xidian University. He has been a Senior Visiting Scholar in the Chinese University of Hong Kong, Hong Kong.

His research interests include array signal processing, space-time adaptive processing, SAR ground moving target indication, and distributed small satellite SAR system design. Dr. Liao is a member of the National Outstanding Person and the Cheung Kong Scholars in China.

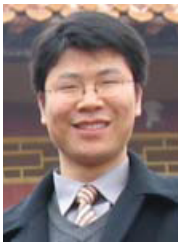

Shengqi Zhu (M'12) was born in Jiangxi. He received the B.S. and Ph.D. degrees in electrical engineering from Xidian University, Xian, China, in 2005 and 2010, respectively.

In 2010 he joined Xidian University as a full assistant professor in National Laboratory of Radar Signal Processing where he was promoted to associate professor in 2012. In 2011 and 2014, he was awarded the Young Scientists Award for Excellence in Scientific Research by the International Union of Radio Science (URSI). Currently, he has been the reviewer for *IEEE Transactions on Aerospace and Electronic Systems*, *IEEE Transactions on Geoscience and Remote Sensing*, *IET Radar Sonar and Navigation* and so on.

His research interests include space-time adaptive processing, multiple-input multiple-output radar, SAR ground moving target indication and sparse signal processing.

Lei Huang (M'07-SM'14) was born in Guangdong, China. He received the B.Sc., M.Sc., and Ph.D. degrees in electronic engineering from Xidian University, Xian, China, in 2000, 2003, and 2005, respectively.

From 2005 to 2006, he was a Research Associate with the Department of Electrical and Computer Engineering, Duke University, Durham, NC. From 2009 to 2010, he was a Research Fellow with the Department of Electronic Engineering, City University of Hong Kong and a Research Associate with the Department of Electronic Engineering, The Chinese University of Hong Kong. From 2012 to 2014, he was a Full Professor with the Department of Electronic and Information Engineering, Harbin Institute of Technology Shenzhen Graduate School. Since November 2014, he has joined the College of Information Engineering, Shenzhen University, where he is currently a Chair Professor. His research interests include spectral estimation, array signal processing, statistical signal processing, and their applications in radar and wireless communication systems.

He is currently an associate editor of *IEEE Transactions on Signal Processing* and editorial board member of *Digital Signal Processing*.